Original Article

Suppression of NLRP3 inflammasome activation by astragaloside IV via promotion of mitophagy to ameliorate radiation-induced renal injury in mice

Yanping Ding[1], Shuning Liu[1], Mengqing Zhang[1], Meile Su[1], Baoping Shao[2]

[1]School of Life Science, Northwest Normal University, Lanzhou, China; [2]School of Life Science, Lanzhou University, Lanzhou, China

Contributions: (I) Conception and design: Y Ding, S Liu, B Shao; (II) Administrative support: Y Ding, S Liu; (III) Provision of study materials or patients: All authors; (IV) Collection and assembly of data: Y Ding, S Liu, B Shao; (V) Data analysis and interpretation: Y Ding, S Liu, M Zhang, M Su; (VI) Manuscript writing: All authors; (VII) Final approval of manuscript: All authors.

Correspondence to: Baoping Shao, PhD. School of Life Science, Lanzhou University, No. 222 South Tianshui Road, Lanzhou 730000, China. Email: shaobp@lzu.edu.cn.

Background: Irradiation (IR) promotes inflammation and apoptosis by inducing oxidative stress and/or mitochondrial dysfunction (MD). The kidneys are rich in mitochondria, and mitophagy maintains normal renal function by eliminating damaged mitochondria and minimizing oxidative stress. However, whether astragaloside IV (AS-IV) can play a protective role through the mitophagy pathway is not known.

Methods: We constructed a radiation injury model using hematoxylin and eosin (HE) staining, blood biochemical analysis, immunohistochemistry, TdT-mediated dUTP nick end labeling (TUNEL) staining, ultrastructural observation, and Western blot analysis to elucidate the AS-IV resistance mechanism for IR-induced renal injury.

Results: IR induced mitochondrial damage; the increase of creatinine (SCr), blood urea nitrogen (BUN) and uric acid (UA); and the activation of NOD-like receptor thermal protein domain-associated protein 3 (NLRP3) inflammasome and apoptosis in renal tissue. AS-IV administration attenuated the IR-induced MD and reactive oxygen species (ROS) levels in the kidney; enhanced the levels of mitophagy-associated protein [PTEN-induced putative kinase 1 (PINK1)], parkin proteins, and microtubule-associated protein 1 light 3 (LC3) II/I ratio in renal tissues; diminished NLRP3 inflammasome activation-mediated proteins [cleaved cysteinyl aspartate-specific proteinase-1 (caspase-1), interleukin-1β (IL-1β)] and apoptosis-related proteins [cleaved caspase-9, cleaved caspase-3, BCL2-associated X (Bax)]; reduced SCr, BUN, and UA levels; and attenuated the histopathological alterations in renal tissue. Conversely, mitophagy inhibitor cyclosporin A (CsA) suppressed the AS-IV-mediated protection of renal tissue.

Conclusions: AS-IV can strongly diminish the activation and apoptosis of NLRP3 inflammasome, thus attenuating the renal injury induced by radiation by promoting the PINK1/parkin-mediated mitophagy. These findings suggest that AS-IV is a promising drug for treating IR-induced kidney injury.

Keywords: Renal injury; astragaloside IV (AS-IV); radiation; mitophagy; PINK1/parkin

Submitted Jun 05, 2023. Accepted for publication Oct 24, 2023. Published online Jan 23, 2024.
doi: 10.21037/tau-23-323
View this article at: https://dx.doi.org/10.21037/tau-23-323

Introduction

In the modern era, people have a higher chance of exposure to radiation in their daily lives in their occupational environment, during the process of receiving diagnosis and treatment, and from accidents (1). Irradiation (IR) promotes the generation of reactive oxygen species (ROS), which are strongly correlated with mitochondrial dysfunction (MD) in exposed cells (2). In a clinical setting, radiation is used in radiotherapy, which may cause damage to tissues such as the liver, brain, kidney, testes, heart, and lungs (3,4). Studies have revealed that ROS production and MD activate the NOD-like receptor thermal protein domain-associated protein 3 (NLRP3) inflammasome (5). Emerging evidence suggests that the NLRP3 inflammasome has a critical role in diabetic nephropathy, hypertensive kidney disease, and IR-induced renal injury (6-8). The NLRP3 inflammasome is a multiprotein complex consisting of NLRP3, apoptosis-associated speck-like protein containing CARD (ASC), and pro-cleaved cysteinyl aspartate-specific proteinase-1 (caspase-1). NLRP3 is typically activated by a variety of dangerous situations. NLRP3 activation recruits the adaptor protein ASC, which, in turn, cleaves and activates caspase-1 to stimulate the maturation of proinflammatory cytokines, such as interleukin-18 (IL-18) and IL-1β.

Mitochondria also figure prominently in apoptosis (9). MD results in cytochrome C (Cytc) secretion into the cytosol, and Cytc forms a complex with apoptotic protease-activating factor-1 and the inactive zymogen of caspase-9. Subsequently, caspase-9 is cleaved and activated, which then activates the key effector protein in the apoptosis protease cascade, caspase-3 (9,10). Evidence suggests that enhanced apoptosis severely injures the kidney and renders it dysfunctional (5,11). Kidneys are often rich in mitochondria due to their high metabolic requirements and the need to detect and respond to oxidative stress and inflammation generated by injuries. MD was demonstrated to strongly regulate progressions of acute kidney injury and chronic kidney disease (12). An accumulating amount of evidence suggests that renal activity is markedly correlated with the PTEN-induced putative kinase 1 (PINK1)- or parkin pathway-mediated autophagy of damaged mitochondria. Under basal conditions, PINK1 is frequently cleaved by the inner mitochondrial membrane protease presenilin-associated rhomboid-like protein (PARL), thus maintaining PINK1 at a relatively low level. When exposed to stress, PINK1 detects MD and then phosphorylates parkin and ubiquitin to activate parkin and generate ubiquitin chains on damaged mitochondria (13). P62 is a well-known selective autophagic cargo receptor that can recognize ubiquitinated mitochondria and interact with microtubule-associated proteins 1A/1B light chain 3B (LC3), thus mediating the autophagic degradation of mitochondria. Hence, eliminating damaged mitochondria by mitophagy may be an effective approach to minimizing mitochondrial ROS accumulation (14). Nevertheless, there is no consensus as to whether mitophagy regulates IR-induced renal injury.

Astragaloside IV (AS-IV), a primary active ingredient of *Astragalus*, has marked antioxidant, anti-inflammatory, and antiapoptotic properties (15). In a previous study, we introduced AS-IV as a potential neuroprotective agent for the prevention of IR-induced brain damage (16,17). Thus far, however, no reports have surfaced regarding a potential protective effect of AS-IV on IR-induced renal injury. In this study, we hypothesized that mitophagy can remove radiation-damaged mitochondria and thus suppress renal injury. In particular, we investigated whether astragaloside IV can ameliorate IR-induced inflammation and apoptosis by regulating mitophagy. We present this article in accordance with the ARRIVE reporting checklist (available at https://tau.amegroups.com/article/view/10.21037/tau-23-323/rc).

Highlight box

Key findings

- Astragaloside IV (AS-IV) suppressed NOD-like receptor thermal protein domain-associated protein 3 (NLRP3) inflammasome activation via promoting mitophagy to ameliorate radiation-induced renal injury in mice

What is known and what is new?

- The kidney is rich in mitochondria, and mitophagy maintains normal renal function by eliminating damaged mitochondria and minimizing oxidative stress. Nevertheless, there is no consensus on whether mitophagy regulates irradiation (IR)-induced renal injury or the effect of AS-IV on regulating mitophagy.
- AS-IV can strongly diminish activation and apoptosis of NLRP3 inflammasome, thus attenuating radiation-induced renal injury by promoting PTEN-induced putative kinase 1 or parkin-mediated mitophagy.

What is the implication, and what should change now?

- AS-IV is a promising drug for treating IR-induced kidney injury.

Methods

Animals and treatments

Overall, 120 C57 male mice, aged between 5–6 weeks, were purchased from the Medical and Laboratory Animal Center of Lanzhou University and housed in pathogen-free conditions at 20–25 ℃ with ad libitum access to food and water. The animals were arbitrarily separated into 6 groups with 20 mice in each group: control (Con), dimethyl sulfoxide (DMSO) solvent, IR, cyclosporin A (CsA) + IR (IR + CsA), IR + astragaloside IV (40 mg/kg) + CsA (IR + CsA + AS-IV), and IR + astragaloside IV (40 mg/kg) (IR + AS-IV). DMSO and AS-IV were intraperitoneally injected for 1 month, and CsA was intraperitoneally injected for 1 week. AS-IV with a purity >98% was obtained from Dalian Meilun Biotechnology Co., Ltd. (Dalian, China), DMSO was purchased from Solarbio (Beijing, China), and CsA was purchased from AbMole Bioscience Inc (Houston, TX, USA). The AS-IV dosages were selected based on previous studies (16,17). After 1 month of administration, Cobalt-60 (^{60}Co) radiation (Lanzhou Weite Radiation Co., Ltd., Lanzhou, China) was used in mice, and the cumulative radiation dose was 8 Gy. The mice were killed via anesthesia or cervical dislocation after IR and each group was divided into two groups. One group of mice (n=10) was deeply anesthetized with pentobarbital sodium (0.3%, 0.2 mL/10 g, ip), blood was collected from the heart, and then the kidneys were collected after fixing with 4% paraformaldehyde perfusion through the heart for blood biochemical analysis, hematoxylin and eosin (HE) staining, TdT-mediated dUTP nick end labeling (TUNEL) staining, and immunohistochemical observation. The other group of mice (n=10) were killed via cervical dislocation for transmission electron microscopy (TEM) observation, frozen section, and Western blot analysis (*Figure 1A*). Experiments were performed under a project license (No. EA2021027) granted by the Institutional Ethics Board of Lanzhou University in compliance with the regulations of Lanzhou University for the care and use of animals. A protocol was prepared before the study without registration.

Blood biochemical analysis

Creatinine (SCr), blood urea nitrogen (BUN), and uric acid (UA) levels were measured as the renal functional indices. The blood was centrifuged at 2,500 cpm for 15 minutes at 4 ℃ to obtain serum samples. These samples were sent to the Wuhan Servicebio Technology Co., Ltd. (Wuhan, China) for further examination.

HE staining

The renal tissues underwent fixation in 4% paraformaldehyde (BL539A, Biosharp Biotechnology Co., Ltd, Jinan, China) and were embedded in paraffin prior to be sliced into sections. They were next dewaxed with xylene and subjected to HE staining. The histomorphology of the renal tissue was observed via light microscopy (Olympus BX53, Tokyo, Japan).

Immunohistochemistry

Immunohistochemical staining was performed as follows: sections were incubated with NLRP3 (bs-10021R; Bioss Antibodies, Woburn, MA, USA), caspase-3 (bs-20364R; Bioss Antibodies), and LC3 (14600-1-AP, Proteintech, Inc., Rosemont, IL, USA) antibodies for 12 hours at 4 ℃. Following a rinse, sections were exposed to biotin-conjugated goat anti-rabbit immunoglobin G (IgG) secondary antibody (BA1003, Boster Bio, Pleasanton, CA, USA), and subsequently, streptavidin-horseradish peroxidase (HRP) (bs-0437P, Bioss Antibodies) conjugation for 2 hours at room temperature (RT). Finally, the sections were stained with DAB (ZLI-9019; ZSGB-BIO, Beijing, China) and hematoxylin before observation under a light microscope.

Observation of TEM

To conduct TEM, renal pieces underwent fixation in 2.5% glutaraldehyde for 12 hours prior to postfixation in 1% osmium tetroxide for 1 hour, dehydration in ethanol, and embedding in Epon 812. Blocks were then sliced into 50-nm-thick sections on a microtome stained with uranyl acetate and lead citrate. The sections were then evaluated under a TEM (Hitachi, Ltd, Tokyo, Japan) at low magnification to identify representative proximal tubules and then analyzed at high magnification.

TUNEL staining

Apoptosis was assessed using TUNEL assay (G1507; Servicebio, Woburn, MA, USA) as per the manufacturer's directions. The sections were dewaxed, dripped with the proteinase K solution, and then incubated in terminal deoxynucleotidyl transferase (TdT) for 2 hours at 37 ℃ in the dark. The slices were next dripped with streptavidin-

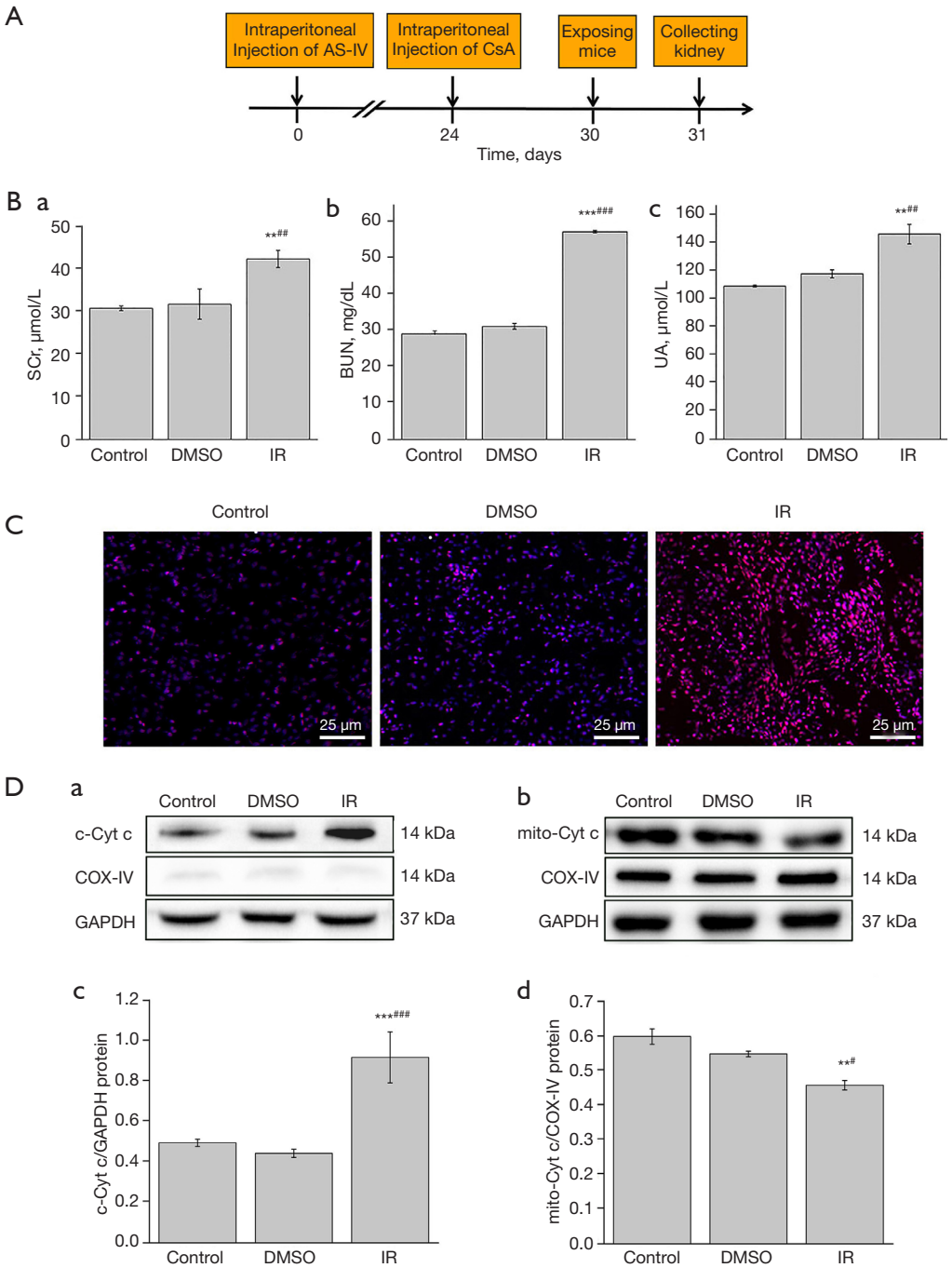

Figure 1 Animal treatment and the effects of radiation on renal function, ROS level, and expression of Cytc. (A) The timeline shows the time points for drug treatment and radiation. (B) SCr (a), BUN (b), and UA (c) levels in different groups of mice are shown. (C) ROS levels in different groups of mouse kidneys were evaluated by dihydroethidium staining (400×). (D) Western blot expression results and the quantification of the levels of Cytc in cytoplasm (a,c) and mitochondria (b,d) in the kidneys of each group, with normalization to GAPDH and COX-IV respectively. The data are expressed as the mean ± standard error of the mean (n=3; **, P<0.01 and ***, P<0.001 *vs.* the control group; #, P<0.05, ##, P<0.01 and ###, P<0.001 *vs.* the DMSO group). ROS, reactive oxygen species; Cytc, cytochrome C; AS-IV, astragaloside IV; CsA, cyclosporin A; SCr, creatinine; BUN, blood urea nitrogen; UA, uric acid; DMSO, dimethyl sulfoxide; IR, irradiation; c-Cyt c, Cytc in the cytosol; COX-IV, Cytc oxidase IV; mito-Cyt c, Cytc in the mitochondria.

HRP solution at 37 ℃ for 30 minutes prior to staining with DAB and hematoxylin. Subsequently, the sections were observed under a light microscope, and representative photographs were imaged and analyzed with Image J software (US National Institutes of Health, Bethesda, MD, USA).

Evaluation of ROS

The ROS fluorescent probe, dihydroethidium (DHE) was used to detect the effect of IR on ROS level in the renal tissue. Frozen sections of renal cortex tissue were created, and ROS activity was detected with a ROS test kit (R001; Vigorous Biotechnology Beijing Co., Ltd, Beijing, China). In brief, autofluorescence quenching agent was added to the frozen sections, which were rinsed with running water for 10 minutes. Each slide was dunked into DHE diluent and then maintained at 37 ℃ for 30 minutes. Subsequently, they were rinsed in phosphate-buffered saline (PBS) three times prior to being mounted on glass slides using a FluorSave reagent with 4',6-Diamidino-2-phenylindole dihydrochloride (DAPI, D9542, Sigma Chemical Co., St. Louis, MO, USA). Finally, sections were photographed using a fluorescence microscope (Zeiss Axio Imager, Oberkochen, Germany). There were five mice per group, and five discontinuous sections per mice were selected for analysis.

Western blot analysis

About 100 mg of renal tissues underwent homogenization in a 10-fold excess amount of ice cold radioimmunoprecipitation assay (RIPA) protein lysis buffer with 1 mmol of phenylmethylsulfonyl fluoride (PMSF). Tissue homogenate was centrifuged at 4 ℃ for 15 min at 13,000 rpm, and the supernatants were obtained and preserved at −80 ℃. In addition, another 100 mg of renal tissues was used to extract mitochondrial and cytoplasmic proteins to detect their expression of cytoplasmic cytochrome C (c-Cytc) according to the manufacturer's instructions (BSP051, Sangon Biotech, Shanghai, China). The supernatant protein concentrations were assessed using a bicinchoninic acid (BCA) kit. The total protein extracts with equal protein concentration were loaded onto 8–15% sodium dodecyl sulfate-polyacrylamide gel electrophoresis (SDS-PAGE) in a gel electrophoresis system before being transferred to a polyvinylidene fluoride (PVDF) membrane using a wet transfer system. This was followed by blocking in 5% skimmed milk in tris-buffered saline with Tween20 (TBST) at RT for 1 h and overnight incubation with primary antibodies against c-Cytc (bs-0013R; Bioss Antibodies), NLRP3, cleaved caspase-1 (bs-10442R; Bioss Antibodies), IL-1β (bs-0812R; Bioss), Bax (A00183; Boster Bio), B-cell lymphoma-2 (Bcl-2; BA0412; Boster Bio), prostacyclin 62 (P62; bs-2951R; Bioss Antibodies), parkin (bs-23687R; Bioss Antibodies), LC3, PINK1 (23274-1-AP; Proteintech), cleaved caspase-3, cleaved caspase-9 (20750S; Cell Signaling Technology, Danvers, MA, USA), Cytc oxidase IV (COX-IV; 11242-1-AP; Proteintech), β-actin (bs-0061R; Bioss Antibodies), and GAPDH (K200057M, Solarbio) at 4 ℃, with subsequent incubation in corresponding HRP-conjugated secondary antibodies at RT for 2 hours. Immunoreactive bands were visualized with an enhanced chemiluminescence kit and the ChemiDoc MP imaging system (Bio-Rad Laboratories, Hercules, CA, USA) prior to quantification with the ImageJ software.

Statistical analysis

Data are expressed as the mean ± standard error of the mean (SEM) and were assessed with SPSS 20.0 software (IBM Corp., Armonk, NY, USA). One-way analysis of variance (ANOVA) was employed to analyze differences between multiple cohorts, and the *t*-test was used to analyze differences between the two cohorts. $P<0.05$ was set as the significance threshold.

Results

Outcomes of IR on renal injury in mice

First, we measured SCr, BUN, and UA as the biochemical indices of renal function to detect the effect of IR on kidneys. As shown in *Figure 1B*, compared with the Con and DMSO mice, the IR mice had significantly higher levels of the SCr ($P<0.01$), BUN ($P<0.001$), and UA ($P<0.01$), but no discernible difference was observed between the Con and DMSO groups.

Mitochondria are one of the main targets when the body is exposed to radiation. Therefore, we evaluated the effect of IR on ROS level in the renal tissue of mice. The results showed that relative to the Con and DMSO groups, the IR group showed markedly enhanced ROS content (*Figure 1C*). Furthermore, Western blot was used to analyze the Cytc released from the mitochondria. The results showed that compared to the Con and DMSO groups, the IR group had significantly elevated levels of

c-Cytc ($P<0.001$) and significantly decreased levels of mitochondrial Cytc ($P<0.01$ and $P<0.05$) (*Figure 1D*). These data indicated that IR induced an increased level of ROS and that Cytc was released from mitochondria to cytoplasm, thus reflecting the occurrence of MD.

Multiple reports have indicated that MD induces inflammatory and apoptotic responses. We detected NLRP3 inflammasome activation-mediated proteins (cleaved caspase-1, IL-1β) and apoptosis-related proteins (cleaved caspase-9, cleaved caspase-3, Bax, and Bcl-2) in renal tissues.

As shown in *Figure 2A*, Western blot analysis revealed that relative to those of the Con and DMSO groups, the IR group had significantly higher expressions of NLRP3 ($P<0.01$ and $P<0.05$), IL-1β ($P<0.001$), cleaved caspase-1 ($P<0.01$), cleaved caspase-9 ($P<0.001$), cleaved caspase-3 ($P<0.001$), and Bax ($P<0.001$), while the level of antiapoptotic Bcl-2 protein was significantly decreased ($P<0.001$). Furthermore, immunohistochemical detection revealed that the positive expressions of both NLRP3 (*Figure 2B*) and caspase-3 (*Figure 2C*) in the IR mice were significantly higher than those in the Con and DMSO mice. The results suggested that IR induced NLRP3 inflammasome activation and apoptosis in renal tissue, possibly causing renal function damage.

AS-IV promoted the mitochondrial autophagosomes and reduced the ROS level in IR-induced renal tissues

TEM was used to observe effect of AS-IV on mitochondria in kidneys after IR exposure. As shown in *Figure 3A*, the TEM results revealed that relative to the Con and DMSO mice, the IR mice mitochondria were swollen and enlarged, and mitochondrial autophagosomes were found. In the IR + AS-IV group, mitochondrial autophagosomes were found.

ROS production is related to impaired mitochondrial function. As depicted in the fluorescence images in *Figure 3B*, relative to the Con and DMSO mice, the IR mice showed markedly enhanced the fluorescence intensity, suggesting ROS formation. Alternately, AS-IV treatment diminished the IR-induced DHE fluorescence. The results indicated that AS-IV attenuated the radiation-induced autophagosomes and ROS level in kidneys.

AS-IV promoted PINK1-/parkin-based mitophagy in IR-induced renal tissue damage

A normal structure of the mitochondria is necessary to maintain the normal cellular metabolism and energy conversion of kidneys. Mitophagy is considered to be an effective means of removing damaged mitochondria (DM) and maintaining normal mitochondrial activity. Several studies have shown that AS-IV can control mitochondrial quality through mitophagy, thus playing a protective role in some diseases (18,19). Therefore, we hypothesized that AS-IV can ameliorate radiation-induced renal impairment by modulating the mitochondrial quality and explored the related mechanism through intervention with AS-IV and the mitophagy inhibitor CsA.

To examine whether AS-IV induces PINK1-/parkin-mediated mitophagy, the expression of LC3, P62, PINK1, and parkin protein levels was assessed in renal tissues (*Figure 4A*). Western blot analysis revealed that compared with the Con and DMSO mice, the IR mice had significantly higher expressions of PINK1 ($P<0.001$), parkin ($P<0.001$) and LC3II/I ($P<0.05$), and significantly lower expression of P62 ($P<0.05$). Furthermore, compared with the IR group, AS-IV treatment significantly increased the levels of PINK1 ($P<0.001$), parkin ($P<0.01$) and LC3II/I ($P<0.001$), and significantly decreased the expression of P62 ($P<0.001$). However, mice administered CsA showed significantly diminished PINK, parkin and LC3II/I as compared to IR mice. Immunohistochemistry results of LC3 showed the same trend (*Figure 4B*).

AS-IV inhibited NLRP3 inflammasome activation in IR-induced renal injury

Studies have suggested that the occurrence of mitophagy may prevent NLRP3 inflammasome activation and minimize mature IL-1β release (5,7). We thus evaluated the effect of AS-IV treatment on the expression of NLRP3 inflammasome components. Based on our results, western blot analysis revealed that compared with the IR group, AS-IV treatment markedly decreased the levels of NLRP3 ($P<0.001$), cleaved caspase-1 ($P<0.01$), and IL-1β ($P<0.001$), while CsA treatment significantly increased the levels of these proteins ($P<0.05$) (*Figure 5A*). Correspondingly, immunohistochemical staining of NLRP3 also showed the same trend (*Figure 5B*).

AS-IV inhibited the apoptosis of IR-induced renal tissues

To investigate whether AS-IV could inhibit the apoptosis in IR-induced renal injury, the expressions of cleaved caspase-3 and cleaved caspase-9 protein were assessed. As shown

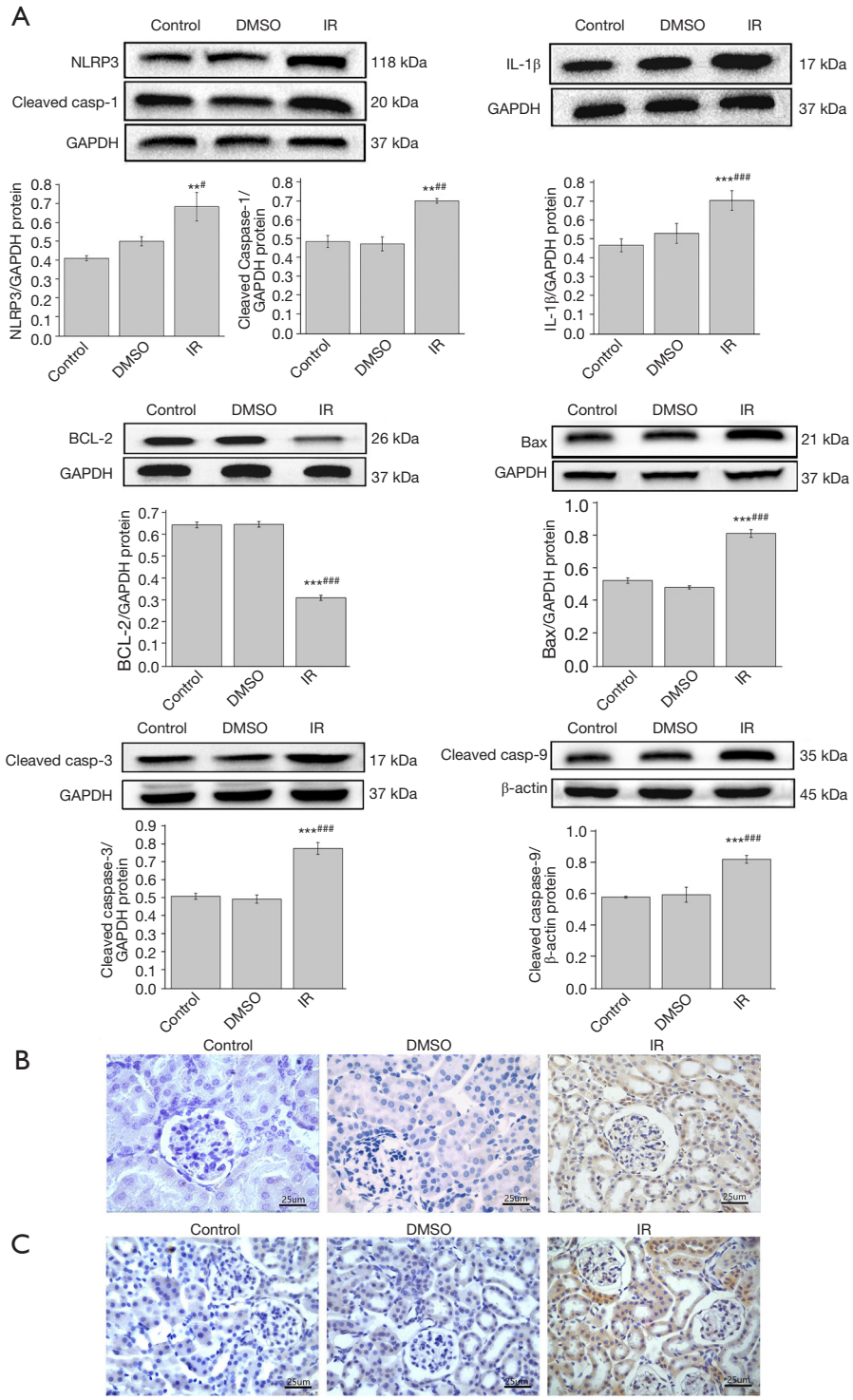

Figure 2 Effects of radiation on the expression of NLRP3 inflammasome and apoptosis in kidneys. (A) Representative immunoblots and quantification of NLRP3, cleaved caspase-1, IL-1β, Bcl-2, Bax, cleaved caspase-3, and cleaved caspase-9 in the renal tissues of each group. (B,C) Representative immunohistochemical staining of the positive expressions of NLRP3 and caspase-3 in the kidney of each group (400×). The data are expressed as the mean ± standard error of the mean (n=3; **, P<0.01 and ***, P<0.001 *vs.* the control group; $^{\#}$, P<0.05, $^{\#\#}$, P<0.01, and $^{\#\#\#}$, P<0.001 *vs.* the DMSO group). DMSO, dimethyl sulfoxide; IR, irradiation.

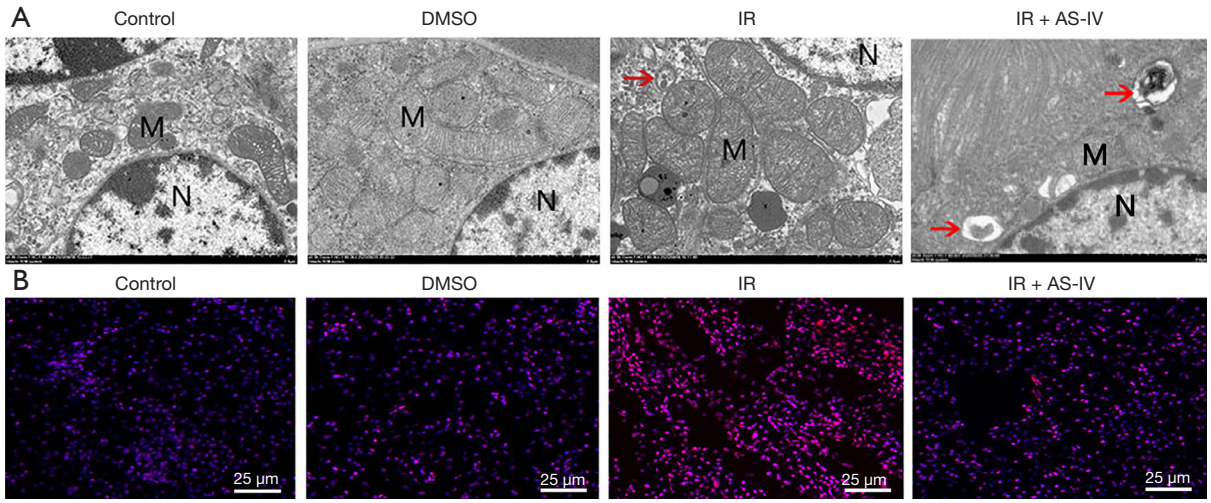

Figure 3 Ultrastructure and ROS level in the renal tissue of each group. (A) AS-IV promoted the mitochondrial autophagosomes in radiation-induced kidney (TEM 2,500×); the letter "N" indicates the nucleolus, the letter "M" indicates the mitochondrion, and the arrow indicates the mitochondrial autophagosome. (B) AS-IV reduced the ROS level in IR kidneys (dihydroethidium staining 400×). ROS, reactive oxygen species; DMSO, dimethyl sulfoxide; IR, irradiation; AS-IV, astragaloside IV; TEM, transmission electron microscopy.

in *Figure 6A*, western blot analysis revealed that cleaved caspase-3 (P<0.001) and cleaved caspase-9 (P<0.01) were drastically reduced in the IR + AS-IV group as compared to the IR group, but CsA treatment significantly reversed this effect. This observation was corroborated by the results of TUNEL staining (*Figure 6B*).

AS-IV attenuated IR-induced renal functional deficits and histopathological changes

The SCr, BUN, and UA levels of each group were examined to elucidate the outcome and mechanism of AS-IV treatment on the recovery of renal function. It was found that relative to IR mice, AS-IV-treated mice showed significantly diminished levels of SCr (P<0.001), BUN (P<0.001), and UA (P<0.01), while these levels were markedly elevated in the IR + CsA mice (P<0.05) (*Figure 7A*). HE staining was used to observe alterations in the renal histomorphology. Based on our results, the IR group mice showed obvious pathological changes in the cortical and medullary zones of the kidneys, including increased capsular space of the glomeruli and dilation of the lumen of the proximal and distal tubules; moreover, some renal tubules showed epithelial cell shedding, dissolution, and hollowing. Compared with the those in the IR group, the renal pathological changes in the IR + AS-IV group mice were significantly improved. The kidneys of IR mice treated with AS-IV showed normal renal corpuscle and tubules (*Figure 7B*).

Discussion

^{60}Co-γ rays are commonly used in the treatment of tumors and cancers, and they can also cause acute damage at the tissue or systemic level (20). Compared with other organs, kidneys are more sensitive to radiation (21). Therefore, it is critical to examine the mechanism of IR-induced renal injury and look for effective preventive measures against it. Studies have shown that radiation, including ^{60}Co-γ rays (22,23), 8-Gy γ rays (24), cesium-137 rays (25,26), and X-rays (27), can cause the impairment of renal function and pathological changes. In our study, compared with the control group, the radiation group exhibited significantly increased oxidative damage of the kidneys (increased malondialdehyde, hydrogen peroxide, and advanced oxidation protein products levels; decreased hydrogen peroxide level and total antioxidant capacity), abnormal renal function indices (increased SCr, BUN, cystatin C, N-Gal, and kidney injury molecule-1 levels), and pathological changes of the kidneys (atrophic and fibrotic glomeruli, extensive degeneration and necrosis of the renal tubular epithelial cells, disappearance of brush edges, and vascular congestion). Our study showed that in the IR mice, the renal cortex showed pathological changes; the levels of SCr, BUN, and UA increased; and the expressions of NLRP3 inflammasome and caspase-3

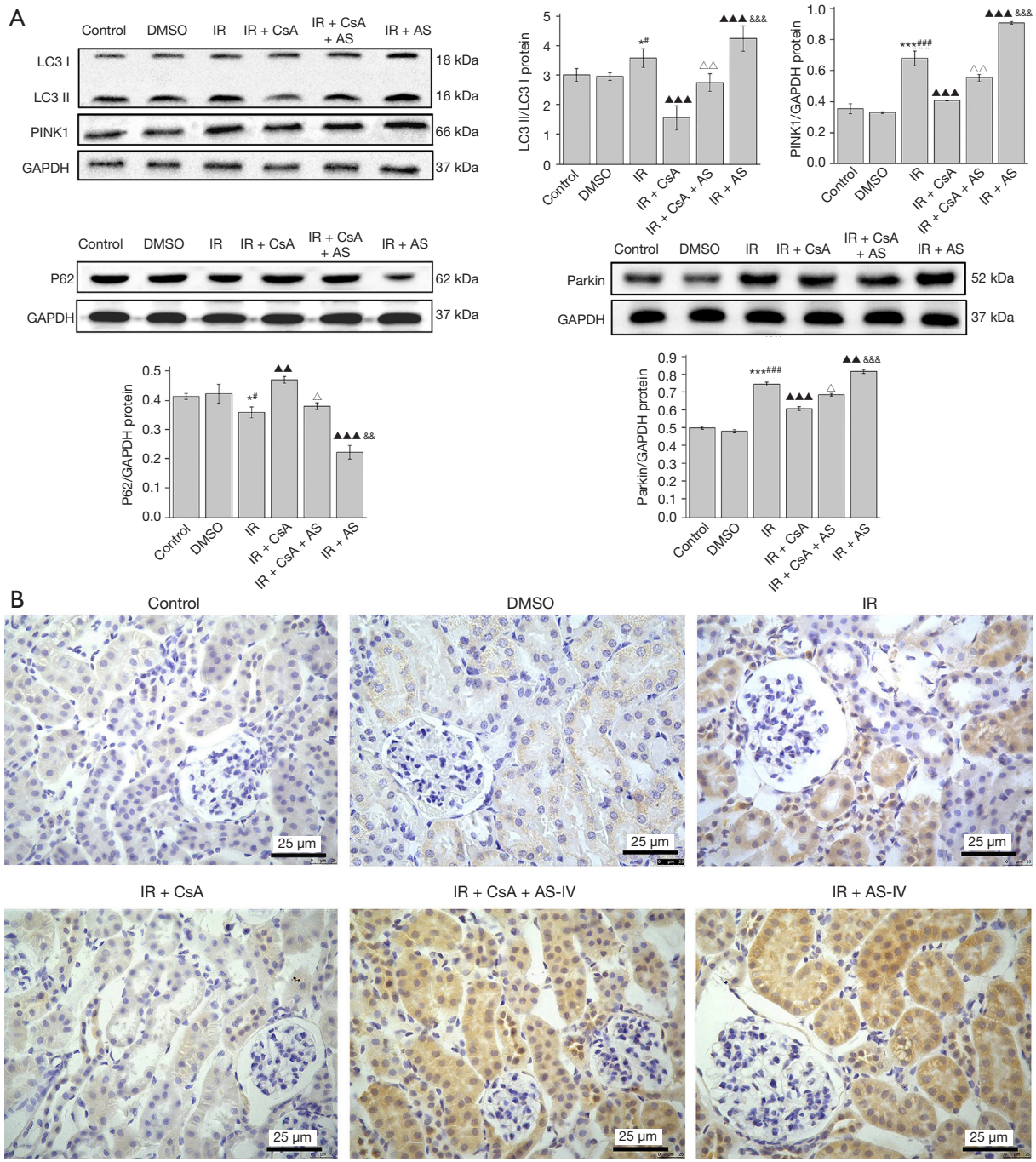

Figure 4 Expression levels of mitophagy-related protein in radiation-induced renal tissues. (A) Representative images of immunoblotting and quantification of the protein levels of LC3, P62, PINK1, and Parkin in the renal tissue of each group. (B) Immunohistochemical staining of the positive expressions of LC3 in the kidney of each group (400×). The data are expressed as the mean ± standard error of the mean (n=3; *, P<0.05 and ***, P<0.001 *vs.* the control group; $^{\#}$, P<0.05 and $^{\#\#\#}$, P<0.001 *vs.* the DMSO group; $^{\blacktriangle\blacktriangle}$, P<0.01 and $^{\blacktriangle\blacktriangle\blacktriangle}$, P<0.001 *vs.* the IR group; $^{\triangle}$, P<0.05 and $^{\triangle\triangle}$, P<0.01 *vs.* the IR + CsA group; $^{\&\&}$, P<0.01 and $^{\&\&\&}$, P<0.001 *vs.* the IR + CsA + AS-IV group). DMSO, dimethyl sulfoxide; IR, irradiation; CsA, cyclosporin A; AS-IV, astragaloside IV; TUNEL, TdT-mediated dUTP nick end labeling.

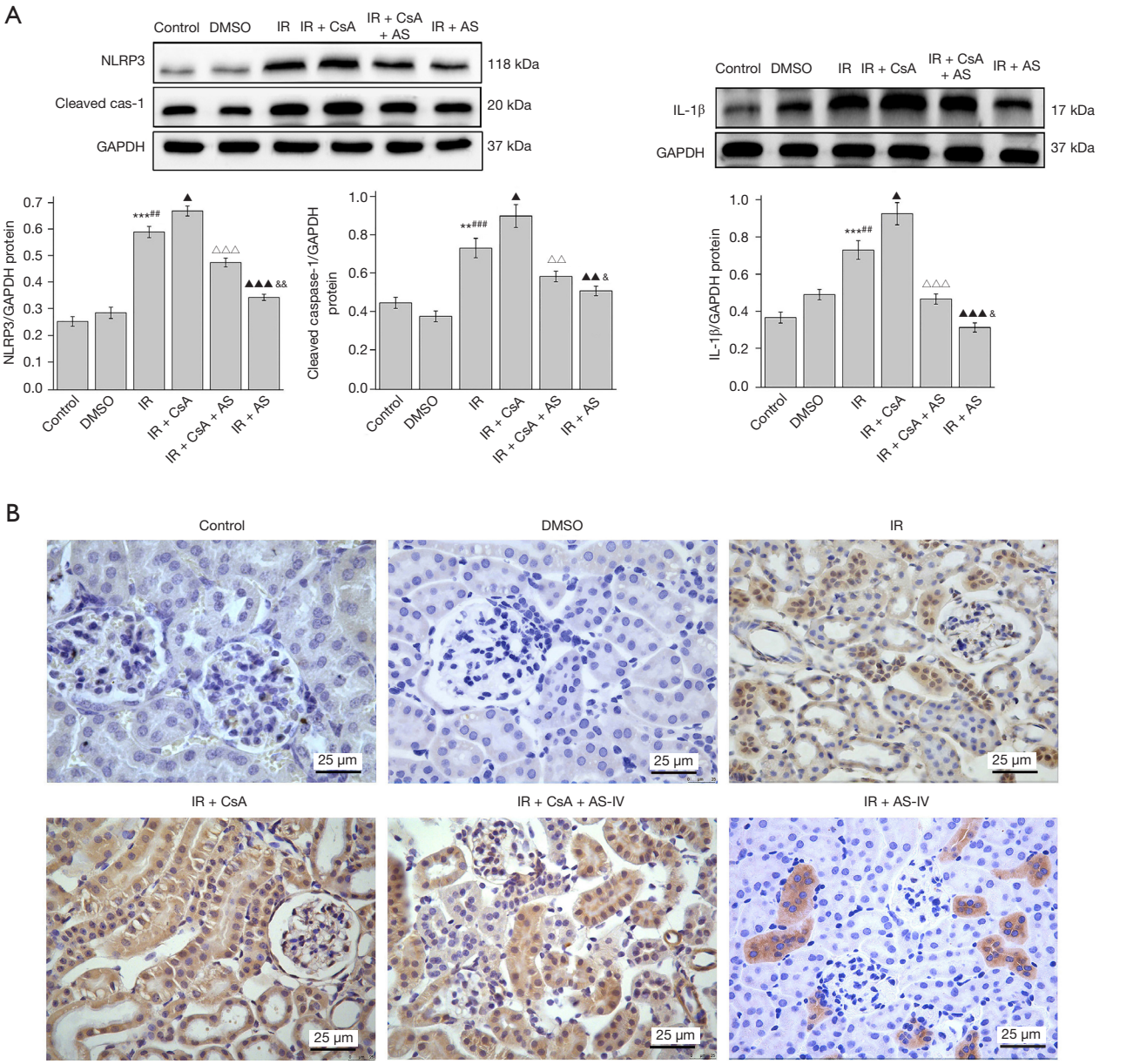

Figure 5 AS-IV inhibited the expression of NLRP3 inflammasome in radiation-induced renal tissues. (A) Representative images of immunoblotting and quantification of the protein levels of NLRP3, caspase-1, and IL-1β in the renal tissues of each group. (B) Immunohistochemical staining of the positive expressions of NLRP3 in the kidneys of each group (400×). The data are expressed as the mean ± standard error of the mean. (n=3; **, P<0.01 and ***, P<0.001 *vs.* the control group; ##, P<0.01 and ###, P<0.001 *vs.* the DMSO group; ▲, P<0.05, ▲▲, P<0.01 and ▲▲▲, P<0.001 *vs.* the IR group; △△, P<0.01, △△△, P<0.001 *vs.* the IR + CsA group; &, P<0.05 and &&, P<0.01 *vs.* the IR + CsA + AS-IV group). DMSO, dimethyl sulfoxide; IR, irradiation; CsA, cyclosporin A; AS-IV, astragaloside IV.

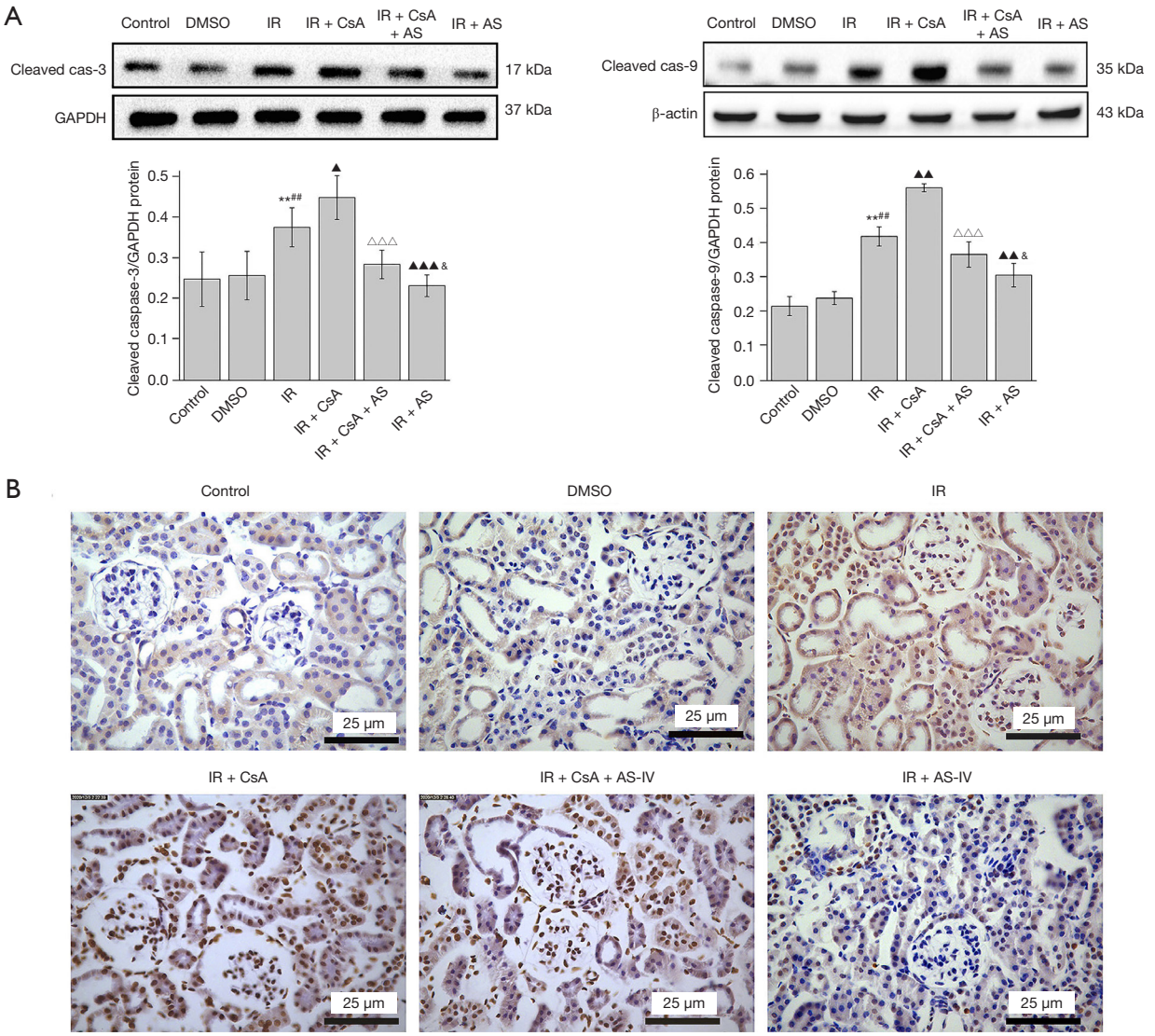

Figure 6 AS-IV inhibited the apoptosis in radiation-induced renal tissues. (A) Representative images of immunoblotting and quantification of caspase-3 and caspase-9 in the renal tissue of each group. (B) TUNEL staining in the kidney of each group (400×). The data are expressed as the mean ± standard error of the mean (n=3; **, P<0.01 *vs.* the control group; ##, P<0.01 *vs.* the DMSO group; ▲, P<0.05, ▲▲, P<0.01 and ▲▲▲, P<0.001 *vs.* the IR group; △△△, P<0.001 *vs.* the IR + CsA group; &, P<0.05 *vs.* the IR + CsA + AS-IV group). DMSO, dimethyl sulfoxide; IR, irradiation; CsA, cyclosporin A; AS-IV, astragaloside IV; TUNEL, TdT-mediated dUTP nick end labeling.

were significantly upregulated. The results indicated that IR can cause inflammatory apoptotic response, resulting in histopathologic damage and renal dysfunction.

In recent years, traditional Chinese medicine has shown considerable effect in preventing and treating radioactive damage. As a natural compound, AS-IV has been identified as having antiradiation, antioxidation, antiinflammation, ant-hypertension, antiapoptosis, and other effects (28,29). Our previous studies suggest that AS-IV can substantially reduce the apoptosis and senescence of brain cells under IR exposure (16,17). Interestingly, recent studies have shown that AS-IV can exert a protective role by regulating mitophagy (18,19). In addition, the literature suggests that AS-IV provides significant protection to multiple renal injury models, including diabetic nephropathy (30) and renal injury induced by cisplatin (28), free fatty acids (31), or tacrolimus (32). Therefore, in this study, we sought to examine whether AS-IV can protect against renal injury

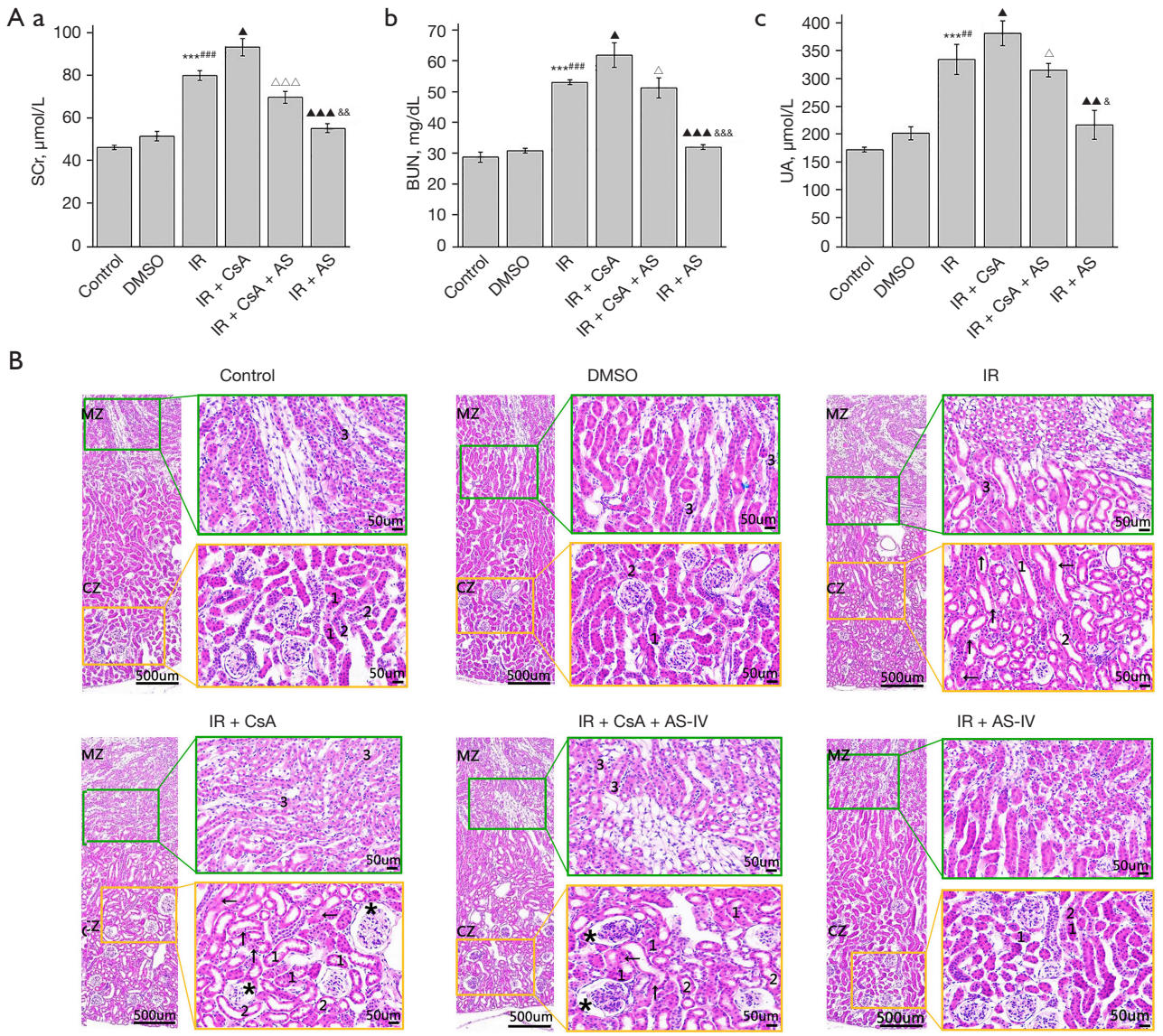

Figure 7 Effects of AS-IV against radiation-induced renal injury. (A) SCr (a), BUN (b), and UA (c) levels in the different groups of mice are shown. (B) Representative micrographs of HE staining of the renal cortex and medulla (100×). "1" indicates the proximal tubule, "2" indicates the distal tubule, "3" indicates the collecting tubule, "*" indicates the increased capsular space of the glomeruli, " ↑ " indicates the cavitation of epithelial cells, " ← " indicates the dissolution and shedding of epithelial cells, the yellow box (200×) indicates the cortical zone (CZ), and the green box (200×) indicates the medullary zone (MZ) (n=3; ***, P<0.001 *vs.* the control group; ##, P<0.01 and ###, P<0.001 *vs.* the DMSO group; ▲, P<0.05, ▲▲, P<0.01, and ▲▲▲, P<0.001 *vs.* the IR group; △, P<0.05 and △△△, P<0.001 *vs.* the IR + CsA group; &, P<0.05, &&, P<0.01, and &&&, P<0.001 *vs.* the IR + CsA + AS-IV group). AS-IV, astragaloside IV; SCr, creatinine; BUN, blood urea nitrogen; UA, uric acid; DMSO, dimethyl sulfoxide; IR, irradiation; CsA, cyclosporin A; HE, hematoxylin eosin staining.

induced by ^{60}Co-γ rays and to clarify its possible mechanism, which, to our knowledge, has not been previously reported.

In this study, we found that AS-IV attenuated IR-induced renal functional deficits and histopathological changes. Under IR exposure of mammalian cells, water radiolysis forms free radicals, which degrade both nuclear DNA and mitochondrial DNA. Excessively damaged mitochondrial DNA and proteins impair mitochondrial activity, which leads to the permanent release of mitochondrial ROS into the whole cell, which, in turn, elicits multiple biological effects (2). During IR, the mitochondria facilitate the bulk of ROS production within cells; in turn, ROS targets mitochondria to cause MD (9). MD results in the release of Cytc into the cytosol (9,10). Consistently, our results showed that in the IR group, Cytc protein expression increased in cytoplasm but decreased in mitochondrial protein, while ROS production increased (*Figure 1*). Therefore, the removal of DM via mitophagy may be an effective strategy for minimizing renal damage caused by oxidative stress (33).

Mitophagy is a process of the selective removal of dysfunctional or redundant mitochondria through autophagy, which has lately become a research hotspot due to its possible role in multiple diseases (34,35). IR-induced MD leads to the activation of mitochondrial autophagy, which degrades dysfunctional mitochondria to maintain cell energy homeostasis (36). Emerging evidence suggests that renal activity is strongly modulated by mitophagy, and abnormal or impaired mitophagy is the core cause of numerous renal diseases (8). The PINK1/parkin pathway mediates the autophagy clearance of DM. Mitophagic deficiency via PINK1 or PARK2 loss has been shown to drastically enhance tubular cell apoptosis and tissue damage, while increasing MD, mitochondrial ROS formation, DNA oxidative injury, and inflammation in several renal injury models (unilateral ureteral obstruction model, contrast/cisplatin media-induced acute kidney injury model, and renal ischemia-reperfusion models) (37-40). Similarly, mitochondrial fragmentation, reduced PINK and Parkin expression, and increased apoptosis were reported to occur in the tubular cells of diabetic nephropathy mice and were then reversed by increasing the expression of PINK1 and parkin via injection of mitoQ (41). In our study, mitophagy was activated to protect renal tissue from IR injury. Furthermore, CsA significantly inhibited the expression of mitophagy markers (PINK1, parkin, and LC3) and aggravated the damage of renal function induced by IR, thereby suggesting the role of mitophagy in the recovery process. In addition, AS-IV was shown to play a protective role by promoting mitophagy, which reduced the accumulation of damaged mitochondria in a vascular senescence model (42). Our results confirmed that AS-IV administration reduced ROS production, enhanced mitophagy, and attenuated the renal functional deficits and histopathological changes induced by IR.

Many investigations have revealed that the upregulation of NLRP3 inflammasome has considerable influence on IR-driven injury, including IR-induced intestinal injury, lung injury, skin reaction, etc. (43). Conversely, reducing NLRP3 has demonstrated a beneficial effect in contrast-induced and cisplatin-induced kidney injury (44,45). Notably, previous research generally suggests that ROS production, lysosome breakdown, and MD can induce NLRP3 inflammasome activation (4). Related reports indicate that mitophagy can be used as an intervention target for NLRP3 inflammasome activation and that promoting mitophagy inhibits the activation of NLRP3 inflammasome (46). Tang *et al.* confirmed that PINK1-/parkin-mediated activation of mitophagy protects against renal ischemia-reperfusion-induced renal injury via the reduction of MD, ROS production, and inflammatory response (47). Lin *et al.* demonstrated that PINK1-/Parkin-mediated mitophagy protects against contrast-induced acute kidney injury by minimizing NLRP3 inflammasome activation (38). Similarly, our analysis revealed that IR-induced renal injury activated NLRP3 inflammasome in mice, while AS-IV treatment significantly diminished NLRP3-caspase-1/IL-1β pathway activation. Consistent with this, CsA treatment significantly reversed this trend, with NLRP3 inflammasome expression being upregulated.

Mitochondria are also critical for regulating cell apoptosis. To determine whether AS-IV can eliminate IR-induced renal damage by increasing mitophagy and thus inhibit apoptosis, we examined the expression of cleaved caspase-9 and caspase-3. Moreover, the degree of neuronal apoptosis was evaluated via TUNEL staining. Our results showed that apoptosis was inhibited through treatment with AS-IV. However, when CsA was administered to inhibit mitophagy, apoptosis increased. Liu *et al.* demonstrated that the PINK1-/parkin-mediated mitophagy offers protection against apoptosis in aluminum-induced kidney damage (11), Hu *et al.* demonstrated that Sal B protects against myocardial ischemic injury by enhancing mitophagy and sustaining mitochondrial activity (48), and Jiang *et al.* demonstrated that PINK1-/parkin-mediated mitophagy reduces palmitic acid-induced apoptosis by minimizing

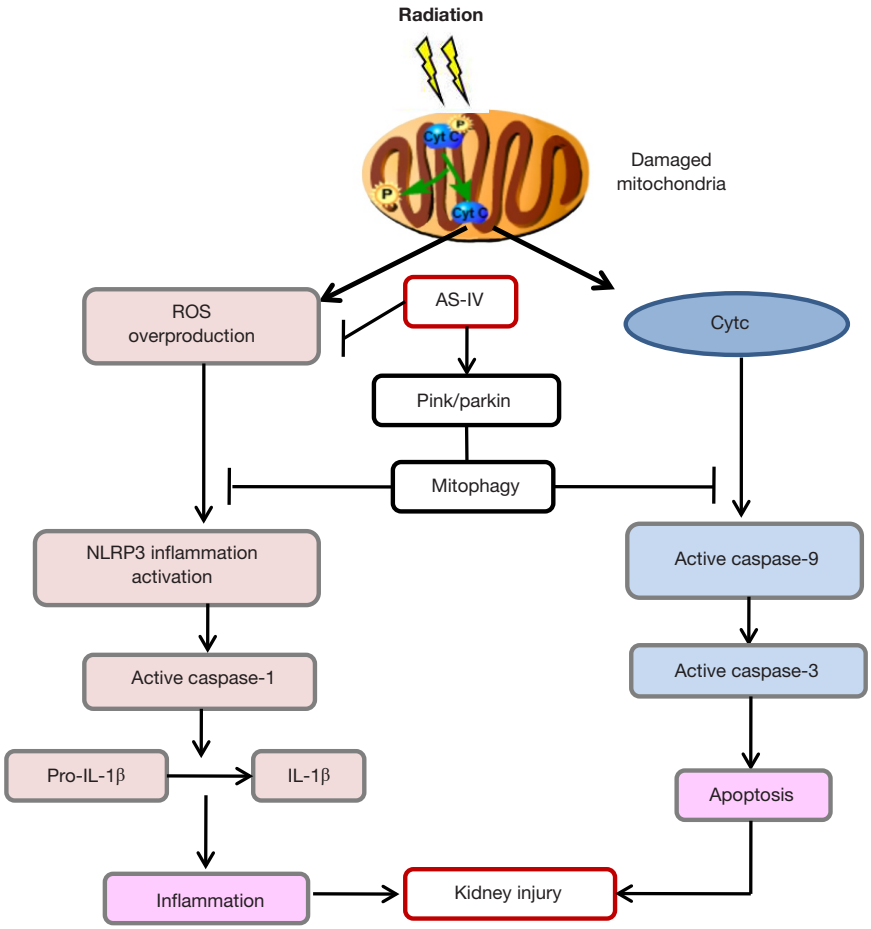

Figure 8 AS-IV markedly diminished NLRP3 inflammasome activation and apoptosis, thus attenuating the kidney injury induced by radiation. AS-IV, astragaloside IV; ROS, reactive oxygen species; Cytc, cytochrome C.

mitochondrial ROS formation (12). Our findings indicate that the activation of PINK1-/parkin-mediated mitophagy protects against apoptosis in kidney damage caused by IR.

Conclusions

Our study demonstrated that ^{60}Coγ IR induced MD of the kidneys, causing mitochondrial Cytc secretion and ROS production, which then activated NLRP3 inflammasome and apoptosis. AS-IV could effectively reduce NLRP3 inflammasome activation and apoptosis in IR-induced kidney injury. The mechanism of the renoprotective effect of AS-IV is correlated with the promotion of clearance of DM via PINK1-/parkin-mediated mitophagy (*Figure 8*). In this study, we focused only on PINK1-/parkin-mediated mitophagy, inflammation, and apoptosis, and thus more research is needed to examine the multitarget effect in detail.

Acknowledgments

Funding: This work was funded by the National Natural Science Foundation of China (No. 31760271), and Gansu Natural Science Foundation (No. 23JRRA714).

Footnote

Reporting Checklist: The authors have completed the ARRIVE reporting checklist. Available at https://tau.amegroups.com/article/view/10.21037/tau-23-323/rc

Data Sharing Statement: Available at https://tau.amegroups.com/article/view/10.21037/tau-23-323/dss

Peer Review File: Available at https://tau.amegroups.com/article/view/10.21037/tau-23-323/prf

Conflicts of Interest: All authors have completed the ICMJE uniform disclosure form (available at https://tau.amegroups.com/article/view/10.21037/tau-23-323/coif). All authors report fundings from National Natural Science Foundation of China (No. 31760271) and Gansu Natural Science Foundation (No. 23JRRA714). The authors have no other conflicts of interest to declare.

Ethical Statement: The authors are accountable for all aspects of the work in ensuring that questions related to the accuracy or integrity of any part of the work are appropriately investigated and resolved. Experiments were performed under a project license (No. EA2021027) granted by the Institutional Ethics Board of Lanzhou University in compliance with the regulations of Lanzhou University for the care and use of animals.

References

1. Batool S, Bibi A, Frezza F, et al. Benefits and hazards of electromagnetic waves, telecommunication, physical and biomedical: a review. Eur Rev Med Pharmacol Sci 2019;23:3121-8.
2. Kawamura K, Qi F, Kobayashi J. Potential relationship between the biological effects of low-dose irradiation and mitochondrial ROS production. J Radiat Res 2018;59:ii91-7.
3. De Ruysscher D, Niedermann G, Burnet NG, et al. Radiotherapy toxicity. Nat Rev Dis Primers 2019;5:13.
4. Nieder C, Milas L, Ang KK. Tissue tolerance to reirradiation. Semin Radiat Oncol 2000;10:200-9.
5. Li X, Gong Y, Li D, et al. Low-Dose Radiation Therapy Promotes Radiation Pneumonitis by Activating NLRP3 Inflammasome. Int J Radiat Oncol Biol Phys 2020;107:804-14.
6. Han Y, Xu X, Tang C, et al. Reactive oxygen species promote tubular injury in diabetic nephropathy: The role of the mitochondrial ros-txnip-nlrp3 biological axis. Redox Biol 2018;16:32-46.
7. Krishnan SM, Ling YH, Huuskes BM, et al. Pharmacological inhibition of the NLRP3 inflammasome reduces blood pressure, renal damage, and dysfunction in salt-sensitive hypertension. Cardiovasc Res 2019;115:776-87.
8. Zuo Z, Jing K, Wu H, et al. Mechanisms and Functions of Mitophagy and Potential Roles in Renal Disease. Front Physiol 2020;11:935.
9. Li X, Fang F, Gao Y, et al. ROS Induced by KillerRed Targeting Mitochondria (mtKR) Enhances Apoptosis Caused by Radiation via Cyt c/Caspase-3 Pathway. Oxid Med Cell Longev 2019;2019:4528616.
10. Hüttemann M, Pecina P, Rainbolt M, et al. The multiple functions of cytochrome c and their regulation in life and death decisions of the mammalian cell: From respiration to apoptosis. Mitochondrion 2011;11:369-81.
11. Liu P, Guo C, Cui Y, et al. Activation of PINK1/Parkin-mediated mitophagy protects against apoptosis in kidney damage caused by aluminum. J Inorg Biochem 2022;230:111765.
12. Jiang XS, Chen XM, Hua W, et al. PINK1/Parkin mediated mitophagy ameliorates palmitic acid-induced apoptosis through reducing mitochondrial ROS production in podocytes. Biochem Biophys Res Commun 2020;525:954-61.
13. Zhao Y, Feng X, Li B, et al. Dexmedetomidine Protects Against Lipopolysaccharide-Induced Acute Kidney Injury by Enhancing Autophagy Through Inhibition of the PI3K/AKT/mTOR Pathway. Front Pharmacol 2020;11:128.
14. Fuhrmann DC, Brüne B. Mitochondrial composition and function under the control of hypoxia. Redox Biol 2017;12:208-15.
15. Li L, Hou X, Xu R, et al. Research review on the pharmacological effects of astragaloside IV. Fundam Clin Pharmacol 2017;31:17-36.
16. Liu X, Shang S, Chu W, et al. Astragaloside IV ameliorates radiation-induced senescence via antioxidative mechanism. J Pharm Pharmacol 2020;72:1110-8.
17. Liu X, Ding Y, Jiang C, et al. Astragaloside IV ameliorates radiation-induced nerve cell damage by activating the BDNF/TrkB signaling pathway. Phytother Res 2023;37:4102-16.
18. Liu X, Wang W, Song G, et al. Astragaloside IV ameliorates diabetic nephropathy by modulating the

mitochondrial quality control network. PLoS One 2017;12:e0182558.
19. Qin S, Yin J, Huang S, et al. Astragaloside IV Protects Ethanol-Induced Gastric Mucosal Injury by Preventing Mitochondrial Oxidative Stress and the Activation of Mitochondrial Pathway Apoptosis in Rats. Front Pharmacol 2019;10:894.
20. Shakyawar SK, Mishra NK, Vellichirammal NN, et al. A Review of Radiation-Induced Alterations of Multi-Omic Profiles, Radiation Injury Biomarkers, and Countermeasures. Radiat Res 2023;199:89-111.
21. Cheema AK, Mehta KY, Rajagopal MU, et al. Metabolomic Studies of Tissue Injury in Nonhuman Primates Exposed to Gamma-Radiation. Int J Mol Sci 2019;20:3360.
22. Kaldir M, Cosar-Alas R, Cermik TF, et al. Amifostine use in radiation-induced kidney damage. Preclinical evaluation with scintigraphic and histopathologic parameters. Strahlenther Onkol 2008;184:370-5.
23. Hormati A, Ahmadpour S, Afkhami Ardekani M, et al. Radioprotective effects of montelukast, a selective leukotriene CysLT1 receptor antagonist, against nephrotoxicity induced by gamma radiation in mice. J Biochem Mol Toxicol 2020;34:e22479.
24. Mahgoub S, Sallam AO, Sarhan HKA, et al. Role of Diosmin in protection against the oxidative stress induced damage by gamma-radiation in Wistar albino rats. Regul Toxicol Pharmacol 2020;113:104622.
25. Abdel-Magied N, Elkady AA. Possible curative role of curcumin and silymarin against nephrotoxicity induced by gamma-rays in rats. Exp Mol Pathol 2019;111:104299.
26. Bellés M, Gonzalo S, Serra N, et al. Environmental exposure to low-doses of ionizing radiation. Effects on early nephrotoxicity in mice. Environ Res 2017;156:291-6.
27. Mercantepe T, Topcu A, Rakici S, et al. The radioprotective effect of N-acetylcysteine against x-radiation-induced renal injury in rats. Environ Sci Pollut Res Int 2019;26:29085-94.
28. Song Y, Hu T, Gao H, et al. Altered metabolic profiles and biomarkers associated with astragaloside IV-mediated protection against cisplatin-induced acute kidney injury in rats: An HPLC-TOF/MS-based untargeted metabolomics study. Biochem Pharmacol 2021;183:114299.
29. Zhang J, Wu C, Gao L, et al. Astragaloside IV derived from Astragalus membranaceus: A research review on the pharmacological effects. Adv Pharmacol 2020;87:89-112.
30. Zhang Y, Tao C, Xuan C, et al. Transcriptomic Analysis Reveals the Protection of Astragaloside IV against Diabetic Nephropathy by Modulating Inflammation. Oxid Med Cell Longev 2020;2020:9542165.
31. Chen Q, Su Y, Ju Y, et al. Astragalosides IV protected the renal tubular epithelial cells from free fatty acids-induced injury by reducing oxidative stress and apoptosis. Biomed Pharmacother 2018;108:679-86.
32. Gao P, Du X, Liu L, et al. Astragaloside IV Alleviates Tacrolimus-Induced Chronic Nephrotoxicity via p62-Keap1-Nrf2 Pathway. Front Pharmacol 2021;11:610102.
33. Bhatia D, Choi ME. The Emerging Role of Mitophagy in Kidney Diseases. J Life Sci (Westlake Village) 2019;1:13-22.
34. Bhatia D, Capili A, Choi ME. Mitochondrial dysfunction in kidney injury, inflammation, and disease: Potential therapeutic approaches. Kidney Res Clin Pract 2020;39:244-58.
35. Bae E, Kim JH, Jung MH, et al. Paricalcitol Attenuates Contrast-Induced Acute Kidney Injury by Regulating Mitophagy and Senescence. Oxid Med Cell Longev 2020;2020:7627934.
36. Wu J, Zhang B, Wuu YR, et al. Targeted cytoplasmic irradiation and autophagy. Mutat Res 2017;806:88-97.
37. Li S, Lin Q, Shao X, et al. Drp1-regulated PARK2-dependent mitophagy protects against renal fibrosis in unilateral ureteral obstruction. Free Radic Biol Med 2020;152:632-49.
38. Lin Q, Li S, Jiang N, et al. PINK1-parkin pathway of mitophagy protects against contrast-induced acute kidney injury via decreasing mitochondrial ROS and NLRP3 inflammasome activation. Redox Biol 2019;26:101254.
39. Zhou L, Zhang L, Zhang Y, et al. PINK1 Deficiency Ameliorates Cisplatin-Induced Acute Kidney Injury in Rats. Front Physiol 2019;10:1225.
40. Livingston MJ, Wang J, Zhou J, et al. Clearance of damaged mitochondria via mitophagy is important to the protective effect of ischemic preconditioning in kidneys. Autophagy 2019;15:2142-62.
41. Xiao L, Xu X, Zhang F, et al. The mitochondria-targeted antioxidant MitoQ ameliorated tubular injury mediated by mitophagy in diabetic kidney disease via Nrf2/PINK1. Redox Biol 2017;11:297-311.
42. Li H, Xu J, Zhang Y, et al. Astragaloside IV alleviates senescence of vascular smooth muscle cells through activating Parkin-mediated mitophagy. Hum Cell 2022;35:1684-96.
43. Wei J, Wang H, Wang H, et al. The role of NLRP3 inflammasome activation in radiation damage. Biomed Pharmacother 2019;118:109217.

44. Li S, Lin Q, Shao X, et al. NLRP3 inflammasome inhibition attenuates cisplatin-induced renal fibrosis by decreasing oxidative stress and inflammation. Exp Cell Res 2019;383:111488.
45. Yang SK, Han YC, He JR, et al. Mitochondria targeted peptide SS-31 prevent on cisplatin-induced acute kidney injury via regulating mitochondrial ROS-NLRP3 pathway. Biomed Pharmacother 2020;130:110521.
46. Song SJ, Kim SM, Lee SH, et al. Rhabdomyolysis-Induced AKI Was Ameliorated in NLRP3 KO Mice via Alleviation of Mitochondrial Lipid Peroxidation in Renal Tubular Cells. Int J Mol Sci 2020;21:8564.
47. Tang C, Han H, Yan M, et al. PINK1-PRKN/PARK2 pathway of mitophagy is activated to protect against renal ischemia-reperfusion injury. Autophagy 2018;14:880-97.
48. Hu Y, Wang X, Li Q, et al. Salvianolic acid B alleviates myocardial ischemic injury by promoting mitophagy and inhibiting activation of the NLRP3 inflammasome. Mol Med Rep 2020;22:5199-208.

Cite this article as: Ding Y, Liu S, Zhang M, Su M, Shao B. Suppression of NLRP3 inflammasome activation by astragaloside IV via promotion of mitophagy to ameliorate radiation-induced renal injury in mice. Transl Androl Urol 2024;13(1):25-41. doi: 10.21037/tau-23-323

